

Optimal Two-Finger Squeezing of Deformable Objects

Yan-Bin Jia Huan Lin Feng Guo

Department of Computer Science

Iowa State University

Ames, IA 50011, USA

jia, linhuan, fguo@iastate.edu

Abstract—This paper gives an in-depth analysis of two-finger squeeze grasping of deformable objects introduced in our previous work [6] with a focus on two special classes: *stable squeezes*, which minimize the potential energy of the system among squeezes of the same magnitude, and *pure squeezes*, which eliminate all possible Euclidean motions from the resulting deformations. Next, the paper characterizes the best resistance by a grasp to an adversary finger under known translation, as the one that minimizes the work done by the grasping fingers. An optimization scheme is offered to deal with the general case of frictional segment contact. Simulation and experimental results are presented.

I. INTRODUCTION

Robot grasping of deformable objects is an under-researched area, for reasons that come from both mechanics and computation. First, during a grasp operation, an object’s global geometry changes, so do the torques even if the exerted forces stay the same. Second, the initial contact points grow into areas, and the contact mode could switch between stick and slip at every point inside such an area.

The focus on force balance in rigid body grasping is no longer justified for deformable body grasping, because the prescribed forces cannot guarantee equilibrium on an initially free object. However, under the classical elasticity theory, during a deformation the applied load and the constraint force balance each other, and the angular momentum is conserved [1, pp. 49–52]. For this reason, our recent work [6] proposed a new paradigm which specifies desired finger displacements instead. In practice, it is also much easier to command a finger to move to a designated position than to control it to exert a prescribed force. After all, force magnitudes are not much of our concern as long as the object can be grasped without causing any irreversible deformation.

Support for this research was provided by the National Science Foundation through the grant IIS-0915876. Any opinions, findings, and conclusions or recommendations expressed in this material are those of the authors and do not necessarily reflect the views of the National Science Foundation. Thanks to the anonymous reviewers for their valuable comments.

In this paper, we will investigate how to characterize the quality of a squeeze grasp proposed in [6]. A successful rigid body grasp must not cause any movement of the contact points. Existing metrics for rigid body grasps are force-centered, either to minimize the possibility of violating some hard constraints [7], [8], to maximize the worst-case adversary force resistible by a “unit” total grasping force [9], [10], or to minimize the maximum finger contact force to resist such an adversary force [2], [3]. We refer to [11] for a comprehensive summary on various grasp metrics.

On a deformable object, the grasping fingers perform some work, most of which is converted into the object’s strain energy via deformation. It therefore makes sense to use an energy-based grasp metric. The deformation-space (D-space) approach [5] characterized the optimal grasp as the one from which the potential energy needed for a release equals the amount at the object’s elastic limit. In this paper, we present two measures: one in terms of stability from the energy point of view, and the other by the amount of work performed by a grasp to resist a disturbing finger under known movement.

The paper uses meter for length, Newton for force, Pascal for pressure, and Joule for work and energy. These units are omitted from now on. In both simulation and experiment, we use Young’s modulus $E = 5 \times 10^4$ Pascal and Poisson’s ratio $\nu = 0.3$.

II. FOUNDATION OF SQUEEZING

We begin with a quick review of our recent work [6] on squeeze grasping of thin $2\frac{1}{2}$ D objects with two fingers. Plane stress is assumed in an object’s cross section, which is discretized into small uniform triangular elements with n vertices $\mathbf{p}_l = (x_l, y_l)^T$, $1 \leq l \leq n$. The origin is placed at the centroid $\sum_{l=1}^n \mathbf{p}_l$.

Under deformation, every node \mathbf{p}_l is displaced by $\delta_l = (\delta_{lx}, \delta_{ly})^T$. Displacement of a point inside a triangular element is interpolated over those of the three nodes of the element. The deformed shape of the object is thus described by $\delta = (\delta_1^T, \dots, \delta_n^T)^T$, referred to

as the *displacement field*. We gather the external forces \mathbf{f}_l exerted on \mathbf{p}_l , $1 \leq l \leq n$, into a $2n$ -vector \mathbf{f} . Minimization of the total potential energy yields the familiar constitutive equation: $K\bar{\boldsymbol{\delta}} = \mathbf{f}$, where K is the shape's stiffness matrix that is positive semi-definite with rank $2n - 3$.

The matrix assumes a spectral decomposition $K = V\Lambda V^T$ with the orthogonal matrix $V = (v_{st}) = (\mathbf{v}_1, \mathbf{v}_2, \dots, \mathbf{v}_{2n})$ and the diagonal matrix Λ defined by the positive eigenvalues $\lambda_1, \dots, \lambda_{2n-3}$ of K . The null space of K is spanned by the following three vectors that represent translations and pure rotation: $\mathbf{v}_{2n-2} = (1, 0, \dots, 1, 0)^T / \sqrt{n}$, $\mathbf{v}_{2n-1} = (0, 1, \dots, 0, 1)^T / \sqrt{n}$, and $\mathbf{v}_{2n} = \mathbf{r} / \|\mathbf{r}\|$, where \mathbf{r} is the component of $(-y_1, x_1, \dots, -y_n, x_n)^T$ that is orthogonal to \mathbf{v}_{2n-2} and \mathbf{v}_{2n-1} .

The grasp strategy introduced in [6] works by specifying the displacements $\bar{\boldsymbol{\delta}}_t$ of m boundary contact nodes \mathbf{p}_t , $t \in \mathbb{I}$. Here, $m = |\mathbb{I}|$. At any node \mathbf{p}_l , $l \notin \mathbb{I}$, $\mathbf{f}_l = \mathbf{0}$.

Denote by $\bar{\mathbf{v}}_l$, $1 \leq l \leq 2m$, the $2m$ -vector that aggregates $v_{2t-1,l}$ and $v_{2t,l}$, for all $t \in \mathbb{I}$, in the increasing index order. Introduce the matrix

$$M = \begin{pmatrix} A & B \\ B^T & \mathbf{0} \end{pmatrix}, \quad (1)$$

where $A = \sum_{l=1}^{2n-3} \frac{1}{\lambda_l} \bar{\mathbf{v}}_l \bar{\mathbf{v}}_l^T$ and $B = (\bar{\mathbf{v}}_{2n-2}, \bar{\mathbf{v}}_{2n-1}, \bar{\mathbf{v}}_{2n})$. It was shown in [6] that the $(2m+3) \times (2m+3)$ matrix M has an inverse when $m \geq 2$:

$$M^{-1} = \begin{pmatrix} C & E \\ E^T & -E^T A E \end{pmatrix}, \quad (2)$$

where C is symmetric and of dimension $2m \times 2m$.

Deformation is unique for $m \geq 2$ under specified $\bar{\boldsymbol{\delta}}_t$, $t \in \mathbb{I}$, and $\mathbf{f}_l = \mathbf{0}$, $l \notin \mathbb{I}$. Apply the same bar notation to select entries with indices $i \in \mathbb{I}$ from the force vector \mathbf{f} and the displacement field $\bar{\boldsymbol{\delta}}$. We have derived

$$\bar{\mathbf{f}} = C\bar{\boldsymbol{\delta}} \quad \text{and} \quad \boldsymbol{\delta} = H\bar{\boldsymbol{\delta}}, \quad (3)$$

for some $2n \times 2m$ matrix H . The submatrix C is referred to as the *reduced stiffness matrix*. The strain energy is

$$U = \frac{1}{2} \bar{\boldsymbol{\delta}}^T C \bar{\boldsymbol{\delta}}, \quad (4)$$

Let \oplus be the direct sum operator over subspaces.

Theorem 1: Suppose $m \geq 2$. The following hold for the submatrices of M in (1) and M^{-1} in (2):

- (i) $\mathbb{R}^{2m} = \text{col}(B) \oplus \text{col}(C)$ where $\text{rank}(B) = 3$.
- (ii) $\mathbb{R}^{2m} = \text{col}(AC) \oplus \text{col}(E)$ where $\text{rank}(E) = 3$.

Proof: The proof makes use of $MM^{-1} = I_{2n+3}$ concerning the values of product matrix's four blocks, which involve matrices A, B, C , and E . Details are omitted for lack of space. ■

III. STABLE AND PURE SQUEEZES

Denoted by $\mathcal{G}(\mathbf{p}_i, \mathbf{p}_j)$ the placement of two fingers \mathcal{F}_1 and \mathcal{F}_2 at the nodes \mathbf{p}_i and \mathbf{p}_j . Here $\mathbb{I} = \{i, j\}$. For clarity of description, in this section we assume that \mathcal{F}_1 and \mathcal{F}_2 are point fingers, and \mathbf{p}_i and \mathbf{p}_j will always stay as the only contact points during a grasp operation by the fingers.

For stability reason we want to determine the unit displacement $\bar{\boldsymbol{\delta}}$ that minimizes the potential energy

$$\Pi = U - \boldsymbol{\delta}^T \mathbf{f} = U - \bar{\boldsymbol{\delta}}^T \bar{\mathbf{f}} = -\frac{1}{2} \bar{\boldsymbol{\delta}}^T C \bar{\boldsymbol{\delta}},$$

by (3) and (4). Because $m = 2$, $\text{rank}(C) = 4 - \text{rank}(B) = 1$ following Theorem 1. It is clear that Π is minimized by a unit vector orthogonal to $\text{col}(B)$. We can easily show that

$$\hat{\mathbf{u}} = \frac{1}{\sqrt{2} \|\mathbf{p}_i - \mathbf{p}_j\|} \begin{pmatrix} \mathbf{p}_j - \mathbf{p}_i \\ \mathbf{p}_i - \mathbf{p}_j \end{pmatrix} \quad (5)$$

is such a unit vector. Indeed, it is the only one corresponding to a grasp because $-\hat{\mathbf{u}}$ pulls at the contacts.

Theorem 2: The matrix C has the form

$$C = \frac{1}{\hat{\mathbf{u}}^T A \hat{\mathbf{u}}} \hat{\mathbf{u}} \hat{\mathbf{u}}^T. \quad (6)$$

Proof: Writing $C = \hat{\mathbf{u}} \mathbf{c}^T$, for some 4-vector \mathbf{c} , we show $\mathbf{c} = \lambda \hat{\mathbf{u}}$ by symmetry of C . Substitute it into $AC + BE^T = I_{2m}$ from $MM^{-1} = I_{2m+3}$, and left multiply both sides to arrive at (5). Details omitted. ■

We refer to a movement of \mathcal{F}_1 and \mathcal{F}_2 specified by $\bar{\boldsymbol{\delta}} = \rho \hat{\mathbf{u}}$, $\rho > 0$, as a *stable squeeze*, so called because it minimizes the system's potential energy among all squeezes of magnitude ρ . Substituting $\bar{\boldsymbol{\delta}} = \rho \hat{\mathbf{u}}$ and (6) into (4), we obtain the strain energy $U_s = \rho^2 / (2 \hat{\mathbf{u}}^T A \hat{\mathbf{u}})$.

Nevertheless, a stable squeeze does not guarantee that the resulting displacement field $\bar{\boldsymbol{\delta}}$ has no rigid body motion component. Since linear elasticity cannot model large rotation, it is sometimes desirable to avoid rotation. A *pure squeeze* at \mathbf{p}_i and \mathbf{p}_j yields no rigid body motion. This is equivalent to $E^T \bar{\boldsymbol{\delta}} = \mathbf{0}$ as we can establish using (3).

By Theorem 1, the set $\text{col}(AC)$ includes all pure squeezes. Since $AC = A \hat{\mathbf{u}} \hat{\mathbf{u}}^T / (\hat{\mathbf{u}}^T A \hat{\mathbf{u}})$ following Theorem 2, we infer that $\text{col}(AC)$ is spanned by $A \hat{\mathbf{u}}$. Let $\hat{\mathbf{v}} = A \hat{\mathbf{u}} / \|A \hat{\mathbf{u}}\|$.

We refer to ρ in a squeeze $\rho \hat{\mathbf{u}}$ or $\rho \hat{\mathbf{v}}$ as the *squeeze depth*. It is different from the relative distance by which one finger moves toward the other during the squeeze.

Fig. 1 compares the effects of the unit stable squeeze $\hat{\mathbf{u}}$ and the unit pure squeeze $\hat{\mathbf{v}}$ on an object¹. While

¹meshed with 517 nodes, including 112 on the boundary

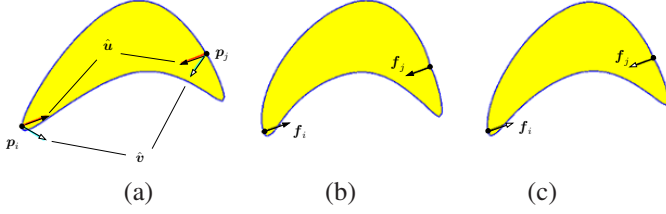


Fig. 1. Comparison between unit stable and pure squeezes: (a) original shape shown with a stable squeeze $\hat{\mathbf{u}} = (0.65923, 0.25577, -0.65923, -0.25577)^T$ (solid black arrowheads) and a pure squeeze $\hat{\mathbf{v}} = (0.79644, -0.49167, -0.20702, -0.28477)^T$ (empty black arrowheads); (b) deformed shape under $\hat{\mathbf{u}}$ with resulting contact forces $\mathbf{f}_i = (0.90772, 0.35218)^T$ and $\mathbf{f}_j = (-0.90772, -0.35218)^T$; (c) deformed shape under $\hat{\mathbf{v}}$ with $\mathbf{f}_i = (0.55243, 0.21433)^T$ and $\mathbf{f}_j = (-0.55243, -0.21433)^T$.

under $\hat{\mathbf{u}}$ the fingers drive the two contact points toward each other, under $\hat{\mathbf{v}}$ they bend the object to prevent any Euclidean motion, in a “clever” way by exerting smaller contact forces.

Translating two fingers \mathcal{F}_1 and \mathcal{F}_2 by δ_i and δ_j , respectively, is equivalent to fixing one finger, say \mathcal{F}_1 , while translating \mathcal{F}_2 by $\delta_j - \delta_i$. The two resulting configurations are identical except for a translation by δ_i . Thus, we call a squeeze stable if it is the same as $\rho\hat{\mathbf{u}}$ up to translation and rotation.

IV. RESISTING AN ADVERSARY FINGER — THE CASE OF FIXED CONTACTS

Consider a grasp $\mathcal{G}(\mathbf{p}_i, \mathbf{p}_j)$. Suppose that an adversary finger \mathcal{A} makes contact with the object at \mathbf{p}_k , and tries to break the grasp via a translation \mathbf{a} . To resist \mathcal{A} , the two grasping fingers \mathcal{F}_1 and \mathcal{F}_2 translate by \mathbf{d}_1 and \mathbf{d}_2 , respectively. We would like to determine \mathbf{d}_1 and \mathbf{d}_2 that result in the minimum efforts by \mathcal{F}_1 and \mathcal{F}_2 in such resistance. This effort is best characterized by the total work done by these two grasping fingers.

The general scenario is depicted in Fig. 2, in which the

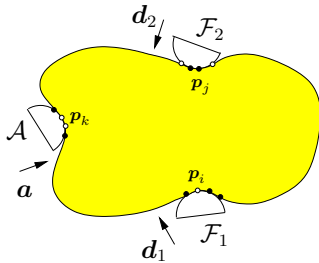


Fig. 2. Resisting a translating adversary finger.

finger contacts have evolved from the nodes $\mathbf{p}_i, \mathbf{p}_j, \mathbf{p}_k$ into segments as $\mathcal{F}_1, \mathcal{F}_2, \mathcal{A}$ translate. Every contact

segment is uniquely represented by a sequence of nodes on it². At an instant during the resistance, \mathcal{F}_1 makes contact with the set of nodes $\{\mathbf{p}_t \mid t \in \mathbb{I}\}$, \mathcal{F}_2 with $\{\mathbf{p}_t \mid t \in \mathbb{J}\}$, and \mathcal{A} with $\{\mathbf{p}_t \mid t \in \mathbb{K}\}$. We can partition the scenario into small periods, within each of which the contact sets $\mathbb{I}, \mathbb{J}, \mathbb{K}$ do not change.

In this section, we will look at fixed point contacts during the resistance, and then generalize to fixed segment contacts. In Section V, we will tackle the general situation with varying $\mathbb{I}, \mathbb{J}, \mathbb{K}$ and contact modes at individual nodes under Coulomb friction.

For clarity of analysis, this section assumes that the three fingers touch the object simultaneously.

A. Fixed Point Contacts

The nodes $\mathbf{p}_i, \mathbf{p}_j$, and \mathbf{p}_k will stay as the only contact points. Deformation of the object is due to their displacements: $\bar{\delta} = (\delta_i^T, \delta_j^T, \delta_k^T)^T = (\mathbf{d}_1^T, \mathbf{d}_2^T, \mathbf{a}^T)^T$.

By (3) the work performed by \mathcal{F}_1 and \mathcal{F}_2 is

$$W_{\mathcal{F}} = \frac{1}{2} \begin{pmatrix} \mathbf{d}_1 \\ \mathbf{d}_2 \\ 0 \end{pmatrix}^T \bar{\mathbf{f}} = \frac{1}{2} \begin{pmatrix} \mathbf{d}_1 \\ \mathbf{d}_2 \\ 0 \end{pmatrix}^T C \begin{pmatrix} \mathbf{d}_1 \\ \mathbf{d}_2 \\ \mathbf{a} \end{pmatrix}. \quad (7)$$

Similarly, for the three fingers, $\bar{\delta}$ is a stable squeeze if $\bar{\delta} \in \text{col}(C)$, and a pure squeeze if $\bar{\delta} \in \text{col}(AC)$. Since $m = 3$, both $\text{col}(C)$ and $\text{col}(AC)$ have three dimensions by Theorem 1.

We first look at the best resistance via a stable squeeze. Consider all \mathbf{d}_1 and \mathbf{d}_2 such that $\bar{\delta} \in \text{col}(C)$, or equivalently, $\bar{\delta} \perp \text{col}(B)$, which is spanned by $(1, 0, 1, 0, 1, 0)^T$, $(0, 1, 0, 1, 0, 1)^T$, and $(-y_i, x_i, -y_j, x_j, -y_k, x_k)^T$. Equivalently, we require

$$\mathbf{d}_1 + \mathbf{d}_2 + \mathbf{a} = \mathbf{0}, \quad (8)$$

$$\mathbf{p}_i \times \mathbf{d}_1 + \mathbf{p}_j \times \mathbf{d}_2 + \mathbf{p}_k \times \mathbf{a} = \mathbf{0}. \quad (9)$$

We substitute (8) into (7) for \mathbf{d}_2 , and rewrite

$$W_{\mathcal{F}} = \frac{1}{2} \mathbf{d}_1^T H \mathbf{d}_1 + \mathbf{c}^T \mathbf{d}_1 + \omega, \quad (10)$$

where H , \mathbf{c} , and ω are constant matrix and vectors depending on \mathbf{a} and C . It is easy to show that H is positive semi-definite.

Denote by $\hat{\mathbf{t}}$ the unit vector in the direction of $\mathbf{p}_i - \mathbf{p}_j$, and $\hat{\mathbf{n}}$ the unit vector such that $\hat{\mathbf{t}} \cdot \hat{\mathbf{n}} = 0$ and $\hat{\mathbf{t}} \times \hat{\mathbf{n}} = 1$. Write $\mathbf{d}_1 = \tau \hat{\mathbf{t}} + \eta \hat{\mathbf{n}}$. Substituting it and (8) into (9), we obtain $\eta \equiv \mathbf{d}_1 \cdot \hat{\mathbf{n}} = (\mathbf{p}_j - \mathbf{p}_k) \times \mathbf{a} / \|\mathbf{p}_i - \mathbf{p}_j\|$. Meanwhile, τ can take on any value.

Substitute $\mathbf{d}_1 = \tau \hat{\mathbf{t}} + \eta \hat{\mathbf{n}}$ into (10), we obtain $W_{\mathcal{F}} = \frac{1}{2} b_2 \tau^2 + b_1 \tau + b_0$, for some b_0, b_1, b_2 , such that $b_2 > 0$.

²under an implicit assumption, consistent with the use of FEM, that a segment always ends at two nodes.

As long as $\mathbf{p}_k \neq \frac{1}{2}(\mathbf{p}_i + \mathbf{p}_j)$,³ the minimum work is $W_{\mathcal{F}}^* = b_0 - b_1^2/(2b_2)$, achieved at $\tau = -b_1/b_2$ by $(\mathbf{d}_1^T, \mathbf{d}_2^T)^T = \|\mathbf{a}\|(\boldsymbol{\psi}_1^T, \boldsymbol{\psi}_2^T)^T$, where $\boldsymbol{\psi}_1$ and $\boldsymbol{\psi}_2$ depend on $\mathbf{p}_i, \mathbf{p}_j, \mathbf{p}_k$ and $\hat{\mathbf{a}}$, the unit direction of \mathbf{a} , only. As \mathcal{A} further translates along $\hat{\mathbf{a}}$, \mathcal{F}_1 and \mathcal{F}_2 just need to translate along the directions of $\boldsymbol{\psi}_1$ and $\boldsymbol{\psi}_2$ proportionally.

Next, we find a pure squeeze that minimizes $W_{\mathcal{F}}$, considering only \mathbf{d}_1 and \mathbf{d}_2 such that $\bar{\boldsymbol{\delta}} \in \text{col}(AC)$. Represent $\bar{\boldsymbol{\delta}} = \tau_1 \hat{\mathbf{u}}_1 + \tau_2 \hat{\mathbf{u}}_2 + \tau_3 \hat{\mathbf{u}}_3$, where $\hat{\mathbf{u}}_1, \hat{\mathbf{u}}_2, \hat{\mathbf{u}}_3$ are the orthogonal unit vectors that span $\text{col}(AC)$. From these two equivalent representations of $\bar{\boldsymbol{\delta}}$, we infer that $\mathbf{a} = (\mathbf{0}, I_2)(\hat{\mathbf{u}}_1, \hat{\mathbf{u}}_2, \hat{\mathbf{u}}_3)(\tau_1, \tau_2, \tau_3)^T$.

In the general case $\text{rank}(Q) = 2$, τ_2 and τ_3 are linear in τ_1 , yielding $W_{\mathcal{F}}$ as a quadratic function of τ_1 . The optimal grasping finger displacements can be obtained from $dW_{\mathcal{F}}/d\tau_1 = 0$. This solution also works for $\text{rank}(Q) = 1$ and $\mathbf{a} \in \text{col}(Q)$, after proper permutation of τ_1, τ_2, τ_3 to set the latter two to zero.

If $\text{rank}(Q) = 1$ and $\bar{\boldsymbol{\delta}} \notin \text{col}(AC)$, the adversary finger cannot be resisted.

B. Fixed Segment Contacts

The displacement $\boldsymbol{\delta}_t$ of a contact node \mathbf{p}_t is \mathbf{d}_1 if $t \in \mathbb{I}$, or \mathbf{d}_2 if $t \in \mathbb{J}$, or \mathbf{a} if $t \in \mathbb{K}$. The vector $\bar{\boldsymbol{\delta}}$ now gathers $\boldsymbol{\delta}_t$, for all $t \in \mathbb{I}$, then for all $t \in \mathbb{J}$, and finally, for all $t \in \mathbb{K}$. Rearrange the rows and columns of the reduced stiffness matrix C introduced in (2) in the same index order as in $\bar{\boldsymbol{\delta}}$.

Again, we first consider stable squeezes, for which the following generalizations of (8) and (9) hold:

$$\sum_{t \in \mathbb{I} \cup \mathbb{J} \cup \mathbb{K}} \boldsymbol{\delta}_t = \mathbf{0} \quad \text{and} \quad \sum_{t \in \mathbb{I} \cup \mathbb{J} \cup \mathbb{K}} \mathbf{p}_t \times \boldsymbol{\delta}_t = \mathbf{0}.$$

The first condition above yields \mathbf{d}_2 in terms of \mathbf{d}_1 and \mathbf{a} . Substitute it into the second condition to yield

$$|\mathbb{I}|(\check{\mathbf{p}} - \check{\mathbf{q}}) \times \mathbf{d}_1 + |\mathbb{K}|(\check{\mathbf{r}} - \check{\mathbf{q}}) \times \mathbf{a} = \mathbf{0}, \quad (11)$$

where $\check{\mathbf{p}} = \frac{1}{|\mathbb{I}|} \sum_{t \in \mathbb{I}} \mathbf{p}_t$, $\check{\mathbf{q}} = \frac{1}{|\mathbb{J}|} \sum_{t \in \mathbb{J}} \mathbf{p}_t$, and $\check{\mathbf{r}} = \frac{1}{|\mathbb{K}|} \sum_{t \in \mathbb{K}} \mathbf{p}_t$ are referred to as the *contact centroids* of the fingers $\mathcal{F}_1, \mathcal{F}_2, \mathcal{A}$, respectively.

As in Section IV-A, we can write the work done by \mathcal{F}_1 and \mathcal{F}_2 into the form of (10), where H , \mathbf{c} , and ω assume new expressions. Minimization parallels that in Section IV-A with a decomposition of \mathbf{d}_1 along the direction $\hat{\mathbf{t}}$ of $\check{\mathbf{p}} - \check{\mathbf{q}}$, and its orthogonal direction $\hat{\mathbf{n}}$.

The case of a pure squeeze with fixed segment contacts also generalizes that of fixed point contacts

³In the degenerate case $\mathbf{p}_k = \frac{1}{2}(\mathbf{p}_i + \mathbf{p}_j)$, $W_{\mathcal{F}}^*$ is achieved by a one-dimensional set of displacements. We may simply let $\tau = -b_1/b_2$.

in Section IV-A. We will end up with a very similar optimization problem. Aside from a different form of $W_{\mathcal{F}}$ and different variables $\tau'_1, \tau'_2, \tau'_3$, over which the constraint is $\mathbf{a} = (\mathbf{0}, I_2)(\hat{\mathbf{u}}'_1, \hat{\mathbf{u}}'_2, \hat{\mathbf{u}}'_3)(\tau_1, \tau'_2, \tau'_3)^T$.

V. FRICTIONAL SEGMENT CONTACTS

We are finally ready to consider optimal resistance with segment contacts under friction. All three fingers, with semicircular tips with radius r , make initial point contacts with the object that will grow into segments as the fingers translate. A contact node may be sticking or sliding on the fingertip. A finger slips on the object if all of its contact nodes are sliding in the same direction. Otherwise, it sticks.

In a realistic scenario, the grasping fingers \mathcal{F}_1 and \mathcal{F}_2 first perform a squeeze on the object by translating toward each other via $s(\mathbf{p}_j - \mathbf{p}_i)$ and $s(\mathbf{p}_i - \mathbf{p}_j)$, for some $s > 0$. Then the adversary finger \mathcal{A} makes contact at the node \mathbf{p}_k and begins a translation \mathbf{a} to try to break the grasp. The system configuration right before this disturbance, including the object's deformed shape and the contact index sets \mathbb{I} and \mathbb{J} for \mathcal{F}_1 and \mathcal{F}_2 , can be determined using the event-based squeeze grasping algorithm from our recent work [6].

Here we modify the above algorithm, which works for two grasping fingers only, by letting the translation distance ρ of \mathcal{A} drive all events. The distance will be sequenced into $\rho_0 = 0 < \rho_1 < \dots < \|\mathbf{a}\|$ such that at every ρ_l , one of the following four contact events happens: contact establishment (A), contact break (B), stick-to-slip transition (C), and slip-to-stick transition (D). Between two events, the contact sets $\mathbb{I}, \mathbb{J}, \mathbb{K}$ do not change.

Consider the moment when \mathcal{A} has translated by the distance ρ_l . For a contact node \mathbf{p}_t , we use $\boldsymbol{\delta}_t^{(l)}$, $\mathbf{f}_t^{(l)}$, and $\theta_t^{(l)}$ to refer to its current displacement, contact force, and polar angle (with respect to the center of the contacting fingertip), respectively.

Next, \mathcal{A} will continue moving by an extra distance ϵ in the direction of \mathbf{a} . Suppose ϵ is small enough such that all contacts and their modes will not change. We determine the extra translations $\Delta \mathbf{d}_1$ by \mathcal{F}_1 and $\Delta \mathbf{d}_2$ by \mathcal{F}_2 to resist this extra movement of \mathcal{A} , via minimizing the extra work done by \mathcal{F}_1 and \mathcal{F}_2 :

$$\Delta W_{\mathcal{F}} = \sum_{t \in \mathbb{I} \cup \mathbb{J}} \Delta \boldsymbol{\delta}_t^T \mathbf{f}_t^{(l)} + \frac{1}{2} \sum_{t \in \mathbb{I} \cup \mathbb{J}} \Delta \boldsymbol{\delta}_t^T \Delta \mathbf{f}_t. \quad (12)$$

In the above, $\Delta \boldsymbol{\delta}_t$ is the extra displacement of the contact node \mathbf{p}_t from $\boldsymbol{\delta}_t^{(l)}$, and $\Delta \mathbf{f}_t$ the change in its contact force from $\mathbf{f}_t^{(l)}$.

During this extra translation period, if a node \mathbf{p}_t , $t \in \mathbb{I} \cup \mathbb{J}$, sticks, then $\Delta \boldsymbol{\delta}_t = \Delta \mathbf{d}_1$ or $\Delta \mathbf{d}_2$. If it slides, then

$\Delta\delta_t$ will be the sum of Δd_1 or Δd_2 , and the node's movement $r \begin{pmatrix} \cos\theta_t - \cos\theta_t^{(l)} \\ \sin\theta_t - \sin\theta_t^{(l)} \end{pmatrix}$ on the tip of \mathcal{F}_1 or \mathcal{F}_2 that it is in contact with. Minimization of $\Delta W_{\mathcal{F}}$ would be over $\Delta\delta_1$ and $\Delta\delta_2$, and the polar angle θ_t of every sliding contact p_t . It can get too inefficient.

We stipulate that the work done on p_t , $t \in \mathbb{I} \cup \mathbb{J}$, due to its sliding, by the contacting finger \mathcal{F}_1 or \mathcal{F}_2 will be significantly less than the amount due to its translation with the finger. Instead of minimizing $\Delta W_{\mathcal{F}}$, we minimize its approximation $\Delta \tilde{W}_{\mathcal{F}}$ by treating every sliding node in contact with \mathcal{F}_1 , \mathcal{F}_2 , or \mathcal{A} as if it would be sticking during the period of the extra resistance period.

In short, whether a contact node p_t sticks or slips, its extra displacement $\Delta\delta_t$ will be set as Δd_1 if $t \in \mathbb{I}$, Δd_2 if $t \in \mathbb{J}$, and $\epsilon \frac{\mathbf{a}}{\|\mathbf{a}\|}$ if $t \in \mathbb{K}$. Then $\Delta d_1 = \epsilon d'_1$ and $\Delta d_2 = \epsilon d'_2$, where d'_1 and d'_2 are determined like d_1 and d_2 in Section IV-B with ϵa replacing a .

The extra translation distance ϵ ends by the occurrence of the next contact event. The four contact events are tested, with every increment of ϵ , using a subroutine from [6]. Such tests must take into account sliding of contact nodes. Once an event occurs, the overall translation distance for \mathcal{A} is updated as $\rho_{l+1} = \rho_l + \epsilon$. In addition to the index sets $\mathbb{I}, \mathbb{J}, \mathbb{K}$, update the set \mathbb{P} of sliding contacts and the set \mathbb{T} of sticking contacts (with any of $\mathcal{F}_1, \mathcal{F}_2$, and \mathcal{A}).

If the adversary finger \mathcal{A} begins to slide after an event, it has been successfully resisted. If either \mathcal{F}_1 or \mathcal{F}_2 starts to slide, the grasp fails to resist \mathcal{A} . If none of the above two cases happens, \mathcal{A} will complete its translation a while being resisted.

Fig. 3(a) shows a convex shape first grasped under a stable squeeze by two fingertips \mathcal{F}_1 (translating via $(-0.00068, 0.002)^T$ from p_i to p_j) and \mathcal{F}_2 (motionless). The fingertip's radius is 0.02. An adversary finger \mathcal{A} starts pushing the object through translation $\mathbf{a} = (0.0024, 0.0044)^T$, as shown in (b). The resistance algorithm generates two trajectories for \mathcal{F}_1 and \mathcal{F}_2 for a stable squeeze shown in (c). Their overall displacements are $d_1 = (-0.0008, -0.0019)^T$ and $d_2 = (-0.0007, -0.0005)^T$. Table I displays the components of the finger forces exerted along the translation directions, at the start and the end of resistance, and the work the fingers have performed. A negative force reading indicates that the contact force influenced by friction was "pulling" away from the translation direction of the finger. Contact events A, B, C, D occurred 7, 0, 3, and 2 times, respectively, during the resistance. The coefficient of contact friction is 0.5.

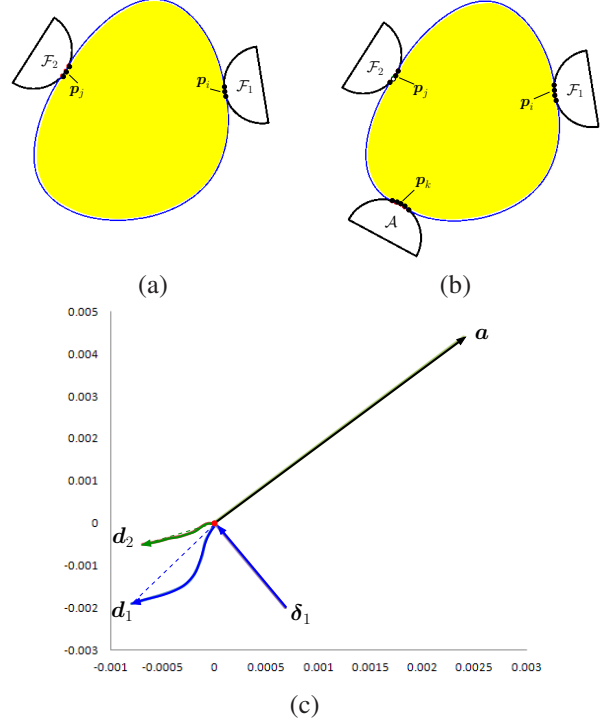


Fig. 3. Resisting an adversary circular fingertip under friction: (a) a convex shape grasped via a stable squeeze; (b) successful resistance to an adversary finger \mathcal{A} ; and (c) trajectories of three fingers during the resistance, translated so their starting points coincide with the origin, and initial trajectory δ_1 of \mathcal{F}_1 before the resistance. Sticking contacts are drawn as solid black circles, while the only sliding contact as a hollow black circle.

| | "optimal" resistance | | |
|---------------|----------------------|-----------------|---------------|
| | \mathcal{F}_1 | \mathcal{F}_2 | \mathcal{A} |
| force (start) | 2.098 | -2.566 | 0 |
| force (end) | 8.136 | -1.23 | 6.57 |
| work | 0.0101 | -0.0017 | 0.0178 |

TABLE I

FORCES EXERTED AND WORK PERFORMED BY THE THREE FINGERS IN FIG. 3 UNDER TRANSLATIONS d_1 , d_2 , AND a .

VI. EXPERIMENT

Fig. 4 shows an experiment that implemented the scenario in Fig. 3. Because the three fingers of our BarrettHand could not be controlled to perform independent translations in the same plane, human hands were involved to hold the fingertips and translate them.

For ease of hand control, the trajectories of \mathcal{F}_1 and \mathcal{F}_2 in Fig. 3 were straightened so they were translating by d_1 and d_2 , respectively, during the resistance. It is referred as the "optimal" resistance, during which \mathcal{F}_2 retreated slightly (i.e., moved away from the object).

We attached a force meter (see Fig. 4(c)) to a finger

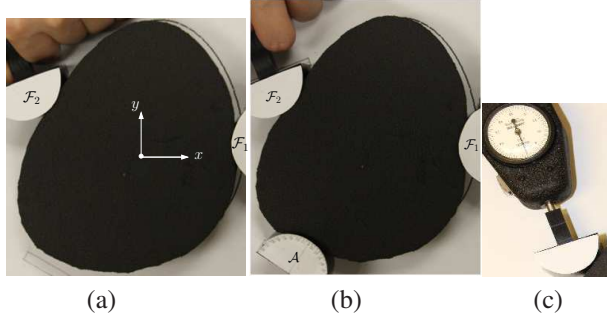


Fig. 4. Experiment on adversary finger resistance: (a) grasp of a rubber foam object of the shape in Fig. 3(a); (b) its resistance to a translating finger \mathcal{A} ; (c) force meter (from Ametek Hunter Spring) attached to a finger for force measurement. The coefficient of contact friction is 0.5.

such that the meter’s axis was aligned with the finger translation. The work done by the finger was estimated as half the product of the translation distance with the sum of the initial and final force readings. The squeeze-and-resistance process was repeated three times, each time with the force meter attached to a different finger. Guided by the trajectories plotted on the platform, the three trials yielded outcomes with slight differences within the acceptable range.

Columns 2 through 4 in Table II display the experimental results. Small discrepancies exist in comparison

| | “optimal” resistance | | | “arbitrary” resistance | | |
|---------------|----------------------|-----------------|---------------|------------------------|-----------------|---------------|
| | \mathcal{F}_1 | \mathcal{F}_2 | \mathcal{A} | \mathcal{F}_1 | \mathcal{F}_2 | \mathcal{A} |
| force (start) | 2.2 | -3.1 | 0 | 6.9 | 4.17 | 0 |
| force (end) | 8.3 | -1.7 | 7.2 | 14.45 | 13.61 | 10 |
| work | 0.011 | -0.002 | 0.018 | 0.045 | 0.032 | 0.025 |

TABLE II
FORCES EXERTED AND WORK PERFORMED BY THE THREE FINGERS IN FIG. 4 UNDER \mathbf{d}_1 AND \mathbf{d}_2 COMPUTED BY THE RESISTANCE ALGORITHM (COLUMNS 2–4) OR ARBITRARILY CHOSEN (COLUMNS 5–7).

with Table I. They were mainly due to several factors: trajectory straightening, measurement errors, and inaccuracy of the human hand pushing.

We also tested an “arbitrary” resistance strategy against the the same adversary finger disturbance. We arbitrarily chose a translation direction $\mathbf{d}_2/\|\mathbf{d}_2\| = (0.447, -0.894)^T$ for \mathcal{F}_2 . To obtain a stable squeeze, we then solved the three equations induced from $(\mathbf{d}_1^T, \mathbf{d}_2^T, \mathbf{a}^T)^T \perp \text{col}(B)$ for \mathbf{d}_1 and the magnitude of \mathbf{d}_2 . The solution was $\mathbf{d}_1 = (-0.004, -0.0012)^T$ and $\mathbf{d}_2 = (0.0016, -0.0032)^T$. Table II shows that much smaller work was carried out by \mathcal{F}_1 and \mathcal{F}_2 with the “optimal” resistance.

VII. DISCUSSION

We investigate several optimality criteria for squeeze grasping of deformable planar objects with two fingers. A stable squeeze minimizes the potential energy for the same amount of squeeze by moving the two fingers toward each other. A pure squeeze ensures that the grasped object undergoes no rigid body motion as it deforms under the finger forces. It prevents large rotations that cannot be described under linear elasticity, on which our analysis is based.

We also look at the best strategy to resist an adversary finger pushing against a grasped object via translation. Our introduced metric is the amount of work performed by the two grasping fingers. Best resistance strategies are analyzed for fixed point and segment contacts. A resistance strategy is developed for rounded fingers under Coulomb friction, by modifying our recent squeeze grasping algorithm [6].

Further investigation and experimental validation need to be conducted for the introduced grasp quality measures. We would also like to explore more the stability of grasping in the presence of disturbances.

REFERENCES

- [1] A. F. Bower, *Applied Mechanics of Solids*, CRC Press, Boca Raton, Florida, 2009.
- [2] S. P. Boyd and B. Wegbreit, “Fast computation of optimal contact forces,” *IEEE Trans. on Robot.*, vol. 23, pp. 1117–1132, 2007.
- [3] M. Buss, L. Faybusovich, and J. Moore, “Dikin-type algorithms for dexterous grasping force optimization,” *Int. J. Robot. Res.*, vol. 17, pp. 831–839, 1998.
- [4] R. H. Gallagher, *Finite Element Analysis: Fundamentals*, Prentice-Hall, Englewood Cliffs, N.J., 1975.
- [5] K. Gopalakrishnan and K. Goldberg, “D-space and deform closure grasps of deformable parts,” *Int. J. Robot. Res.*, vol. 24, pp. 899–910, 2005.
- [6] F. Guo, H. Lin, and Y.-B. Jia, “Squeeze grasping of deformable planar objects with segment contact and stick/slip transitions,” in *Proc. IEEE Int. Conf. Robot. Autom.*, 2013, pp. 3721–3726.
- [7] J. Kerr and B. Roth, “Analysis of multifingered hands,” *Int. J. Robot. Res.*, vol. 4, pp. 3–17, 1986.
- [8] Z. Li and S. S. Sastry, “Task-oriented optimal grasping by multifingered robot hands,” *IEEE J. Robot. Automat.*, vol. 4, pp. 32–44, 1988.
- [9] X. Markenscoff and C. H. Papadimitriou, “Optimum grip of a polygon,” *Int. J. Robot. Res.*, vol. 8, pp. 17–29, 1989.
- [10] B. Mirtich and J. Canny, “Easily computable optimum grasps in 2-D and 3-D,” in *Proc. IEEE Intl. Conf. Robot. Autom.*, 1994, pp. 739–741.
- [11] B. Mishra, “Grasp metrics: optimality and complexity,” in *Algorithmic Foundations of Robotics*, K. Goldberg et al. (ed.), pp. 137–165. A. K. Peters, Boston, MA, 1995.
- [12] B. Mishra, J. T. Schwartz and M. Sharir, “On the existence and synthesis of multifinger positive grips,” *Algorithmica*, vol. 2, pp. 541–558, 1987.